Alkali Metal Cation Effects on Dinitrogen Complexes and Organometallic Compounds

Ryan S. Donnelly and Patrick L. Holland

Department of Chemistry, Yale University, 225 Prospect St., New Haven, Connecticut 06520

Abstract

Alkali metal (AM) cations are often taken for granted as counterions in coordination chemistry and organometallic reactions. However, the AM cation can be more than a bystander in inorganic transformations. This Account focuses on research that has elucidated several types of AM cation effects and how these can be exploited to achieve novel structures and reactivity pathways. A particular focus is on AM cation effects in low-coordinate iron β-diketiminate complexes, though we address general trends and potential applications in systems with other supporting ligands.

The Account is organized by several recurring motifs and trends in how AM cations interact with transition-metal compounds: 1) the AM cations can stabilize and favor the formation of N_2-bridged compounds, 2) the choice of AM cations can influence N–N bond cleavage, 3) the AM cations can influence other bond forming and cleaving reactions, and 4) AM cations can affect ligand binding modes and electronic structure at the metal center. Various methods including X-ray crystallography, density functional theory (DFT) calculations, Mössbauer spectroscopy, vibrational spectroscopy, are leveraged to show how the AM cation affects a given system.

The results of these studies have more general lessons as well. They offer insights into how ligand design can be leveraged to promote or discourage AM cation interactions. AM cations can be used to activate challenging bonds and/or stabilize highly reactive species. The cooperative interactions

described in this Account may offer new paths to reactivity in organometallic chemistry and small molecule activation.

Key References

- McWilliams, S. F.; Rodgers, K. R.; Lukat-Rodgers, G.; Mercado, B. Q.; Grubel, K.; Holland, P. L. Alkali Metal Variation and Twisting of the FeNNFe Core in Bridging Diiron Dinitrogen Complexes. *Inorg. Chem.* **2016**, *55*, 2960–2968.[1]

- Grubel, K.; Brennessel, W. W.; Mercado, B. Q.; Holland, P. L. Alkali Metal Control over N–N Cleavage in Iron Complexes. *J. Am. Chem. Soc.* **2014**, *136*, 16807–16816.[2]

- MacLeod, K. C.; Menges, F. S.; McWilliams, S. F.; Craig, S. M.; Mercado, B. Q.; Johnson, M. A.; Holland, P. L. Alkali-Controlled C–H Cleavage or N–C Bond Formation by N_2-Derived Iron Nitrides and Imides. *J. Am. Chem. Soc.* **2016**, *138*, 11185–11191.[3]

- McWilliams, S. F.; Broere, D. L. J.; Halliday, C. J. V.; Bhutto, S. M.; Mercado, B. Q.; Holland, P. L. Coupling Dinitrogen and Hydrocarbons through Aryl Migration. *Nature* **2020**, *584*, 221–226.[4]

Introduction

Alkali metal (AM) cations are ubiquitous in chemical reactions, and they are usually viewed as spectators used primarily for charge balancing purposes. In spite of this perception, AM cations can play active roles in controlling chemical and biological transformations. For example, organisms have evolved to use AM cations to regulate biological activities, such that enzymatic processes can be promoted or blocked through the presence or absence of these cations. The

cation's role in binding with the protein or substrate can be broadly described as either a cofactor where the cation participates in the active site or as an allosteric promoter where the association alters the protein tertiary structure (**Figure 1**).[5] Examples of these AM cation dependent proteins are pyruvate kinase, ribokinase, and fructose-1,6-bisphosphate aldolase.[6,7]

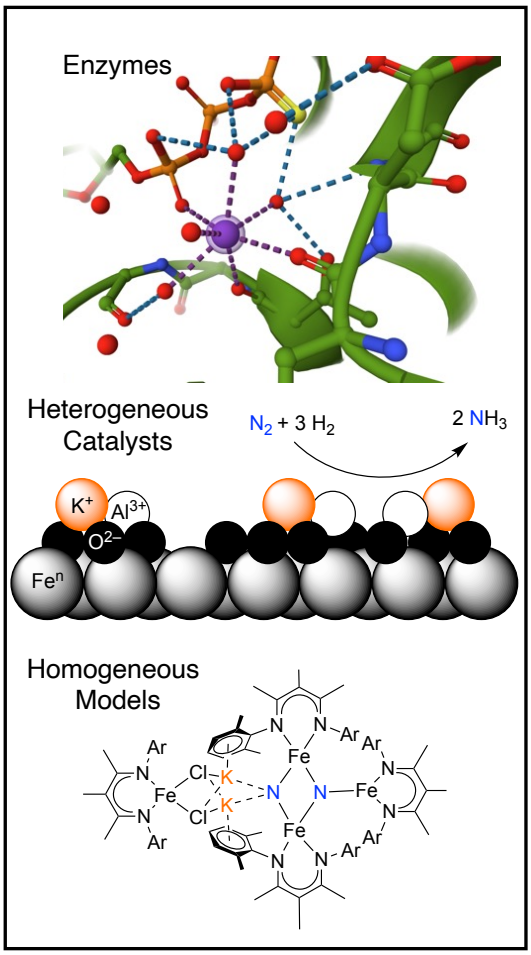

Figure 1. Alkali metal (AM) cations in nature,[8] catalysis,[9] and synthetic chemistry.[10]

Learning from nature, chemists have leveraged AM cations in applications ranging from the regulation and treatment of bipolar disorder to catalysis in large scale industrial processes.[9,11,12] One example of the industrial applications of AM cations is as promoters in the Haber–Bosch (HB) process. During the HB process, dinitrogen (N_2) and dihydrogen (H_2) are converted to ammonia

over a heterogeneous iron (Fe_3O_4) catalyst containing calcium, magnesium, aluminum, and potassium additives.[9,13] The K^+ has a larger ionic radius than the other cationic additives, and accordingly it remains localized on the surface and acts as an electronic promoter that localizes electron density at the surface to aid with H_2 and N_2 adsorption and NH_3 desorption.[13]

Today's chemists seek to understand how else AM cations can promote known reactions and access novel transformations. For example, AM cation effects are being investigated in electrocatalytic reactions for CO_2 reduction and CO reduction.[14,15] Here, we focus on homogeneous complexes, because they offer the opportunity to systematically identify, study, and quantify AM cation effects. Indeed, AM cations have been shown to direct the formation of supramolecular complexes, (de)activate homogeneous catalysts, and affect redox potentials.[16–18]

This Account focuses on our group's experience with understanding and leveraging AM cation effects for organometallic transformations. Most of the reaction sequences revolve around iron complexes bearing β-diketiminate supporting ligands (**Figure 2**). We discovered that these bulky bidentate ligands enable the isolation of a variety of low-coordinate iron complexes, defined as having coordination numbers of three or four.[19] In the quest to use these iron complexes for the activation of strong bonds, we were interested in synthesizing low-valent iron complexes, and it was natural to use AM^0 reductants. However, in many cases these are not simple reducing agents, as the products often incorporate a variety of interactions with the resultant AM^+ cations, which have important influences on the structures, potentials, charge localization, and reactivity of products. This Account describes the types of influences that we have observed from AM cations, with occasional reference to relevant work by other groups.

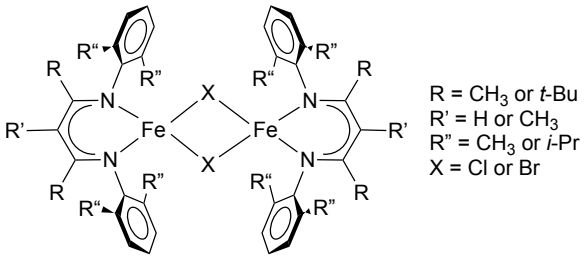

Figure 2. General structure of iron β-diketiminate complexes.[19]

Alkali Metal Cation Effects on Dinitrogen Complexes

The first systems in which we observed AM^+ binding were diiron complexes with bridging N_2. These arose from AM^0 reduction of β-diketiminate-supported iron(II) halide complexes $[LFeX]_2$ (L = β-diketiminate; X = Cl or Br) to the formal iron(0) level (**Scheme 1**).[1] The expulsion of the halides left highly unsaturated iron sites, which bound N_2 in an end-on/end-on mode to give a dianionic LFeNNFeL unit. The use of the AM^0 reductant gave an AM cation that can fit in a pocket between the arenes of two ligands. In this position, the cation forms cation–π interactions with the aryl groups of the β-diketiminate and also interacts with the π system of the bound N_2. Considering the lengthened N=N bonds in the system (>1.2 Å), it is most accurate to consider the bridging dinitrogen as N_2^{2-},[20] further explaining the affinity of the cationic AM^+ for the core.

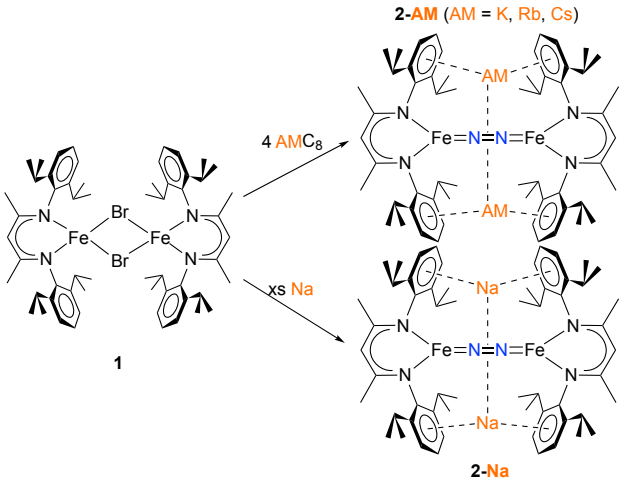

Scheme 1. Reduction of diiron(II) precursor **1** to generate N_2-bridged diiron(0) complexes **2-AM**.[1]

However, different AM^+ are different sizes (**Table 1**), so it is not obvious how they all could fit in the same cavity. Interestingly, the LFeNNFeL core accommodates the different sizes by twisting along the MNNM axis. With Na^+, the β-diketiminates are coplanar, minimizing the distance between the aryl rings. With the much larger Cs^+, the β-diketiminate planes rotate to create a larger pocket, and K^+ and Rb^+ are intermediate in both size and twisting (**Figure 3**). As the dihedral angle increases, the FeNNFe core remains relatively unaffected, maintaining similar Fe–N and N–N bond lengths, and the N–N stretching frequencies are also similar.

Cation	**Ionic Radius (Å)**	**z/r (*e* Å^{-1})**
Li^+	0.76	1.32
Na^+	1.02	0.98
K^+	1.38	0.72
Rb^+	1.52	0.66
Cs^+	1.67	0.60

Table 1. Ionic radii and charge-to-size (z/r) ratio of the alkali metal cations.[21]

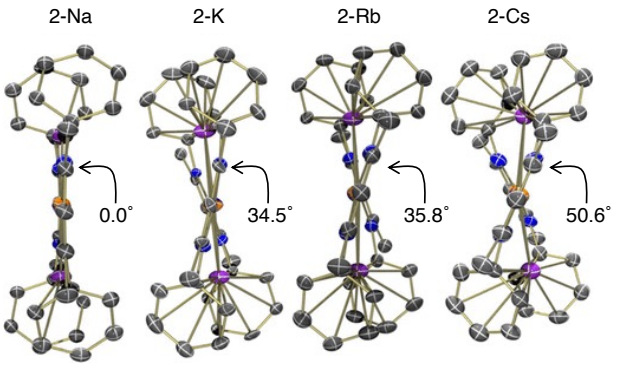

Figure 3. End-on views of **2-AM,** illustrating the twisting of the FeNNFe core. Torsion angles between Fe-(β-diketiminate) planes are shown. Isopropyl groups and hydrogens have been omitted for clarity. Thermal ellipsoids are drawn at 50% probability. Reproduced from ref 1. Copyright 2016 American Chemical Society.

A similar insensitivity to cation identity was observed by Limberg and co-workers for related nickel β-diketiminate complexes incorporating Na^+ and K^+ (**Scheme 2**).[22] The bond distances to both arene centroid and the N_2 unit decrease from K^+ to Na^+, which can be attributed to the decrease in ionic radii of the respective cations. Throughout the changes to both AM^+ and coordination environment, the N–N bond length and resonance Raman frequencies vary minimally (1.185–1.195 Å and 1685–1696 cm^{-1} respectively). The cation identity has a small effect on the dihedral angle between the ligand backbones, which is 32° and 36° for Na^+ and K^+ respectively. Overall, these studies show that the aryl substituents on β-diketiminates offer the opportunity for AM^+ to bind near the iron center and its ligands. The choice of AM^+ can induce geometric changes in the secondary coordination sphere to create an optimal binding pocket, while leaving the TM center relatively unaffected.

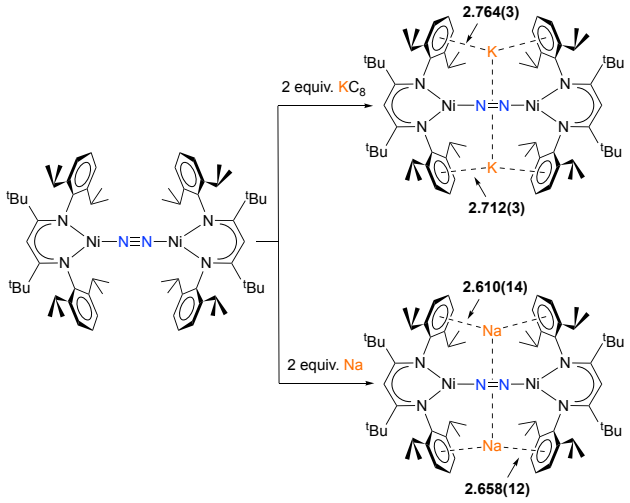

Scheme 2. Synthesis of [NiNNNi]AM$_2$ complexes, highlighting the distances from the AM to the arene centroid.[22]

AM cations can also affect the extent of backbonding to bound N_2. From left to right across the TM series, the *d* orbital energies of the metal center decrease, leading to less backdonation into available π^* orbitals. This trend is well-documented in TM carbonyl complexes, and similarly, the neutral dicobalt(I) LCoNNCoL (**4-Co**) complex exhibits less lengthening/weakening of the N–N bond than the corresponding neutral diiron system **4-Fe** (**Scheme 3**).[23] However, two-electron reduction of LCoNNCoL with potassium graphite (KC_8) gave a dicobalt(0) species **5** with lengthening of the N–N bond from 1.139(2) to 1.220(2) Å, which is on par with the diiron complex.

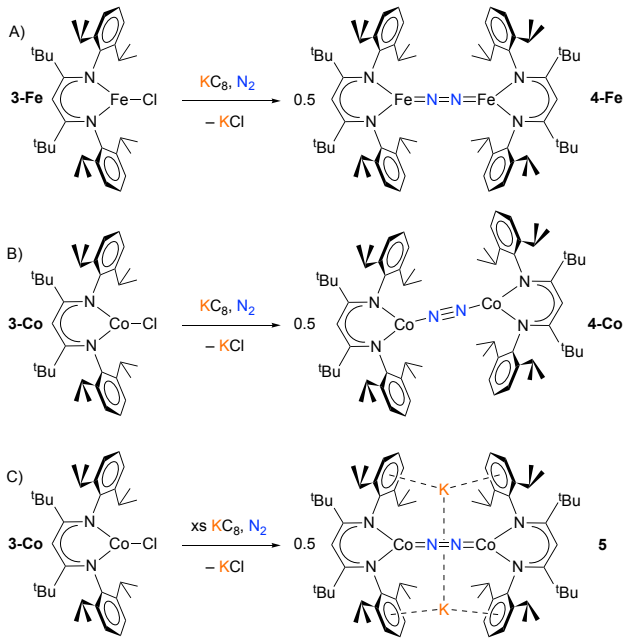

Scheme 3. Formation of MNNM complexes bearing bulky β-diketiminate ligands.[23] A) The neutral FeNNFe complex has a Y-shaped geometry at the transition metal and a lengthened N–N bond. B) The neutral CoNNCo analogue has a T-shaped geometry at the transition metal and a short N–N bond. C) Reduction of the cobalt and incorporation of K^+ leads to N–N lengthening and Y-shaped Co sites.

We attributed this to the incorporation of two potassium cations, each interacting with two Dipp rings and the bound N_2 like in the iron complexes described above. We further hypothesized that the presence of the positive charge pulls electron density into the dinitrogen subunit. In order to test if the AM^+ contributes to the bond weakening, DFT calculations were performed on a simplified system (the β-diketiminate was modelled as $C_3N_2H_5^-$ for computational ease).[23] NBO analyses showed more electron transfer from Co to N_2 when K^+ ions are included in the model.

Thus, AM cations can also work synergistically with poorly backbonding late TMs such as cobalt to enhance their ability to donate electron density to π-accepting ligands like N_2.

In addition to stabilizing N_2-bridged complexes through cation-π interactions, AM cations can also pre-organize metal centers to facilitate reactivity with N_2. This can take advantage of the preference of AM^+ to bind to Lewis basic donors, not just π systems but also lone pairs on hard Lewis bases. For example, ethereal solvents commonly are found to complete the coordination sphere of the AM^+. Further, chelates containing multiple Lewis basic sites such as crown ethers and cryptands may chelate to the AM^+ ion, partially or completely sequestering it.[24,25] In the case of K_2[LFeNNFeL] species described above, we found that the addition of 18-crown-6 under N_2 chelated the K^+ ions and this led to complete disruption of the bridge to yield monomeric [K(18-crown-6)][LFe(N_2)$_2$].[26] Thus, the chelates disrupt the pre-organization of the core, and when the cations become outer-sphere, the core structure comes apart.

We later found a different type of pre-organization when studying the KC_8 reduction of an iron(II) complex bearing a phenoxide ligand (**6, Scheme 4**). Reduction of the starting iron(II)–phenoxo complex **6** with KC_8 furnished monomeric iron(I) products when the K^+ was bound by ethereal solvent, crown ether, or cryptand (**7-K, 7-crown, 7-crypt**).[27] None of these compounds reacted with N_2.

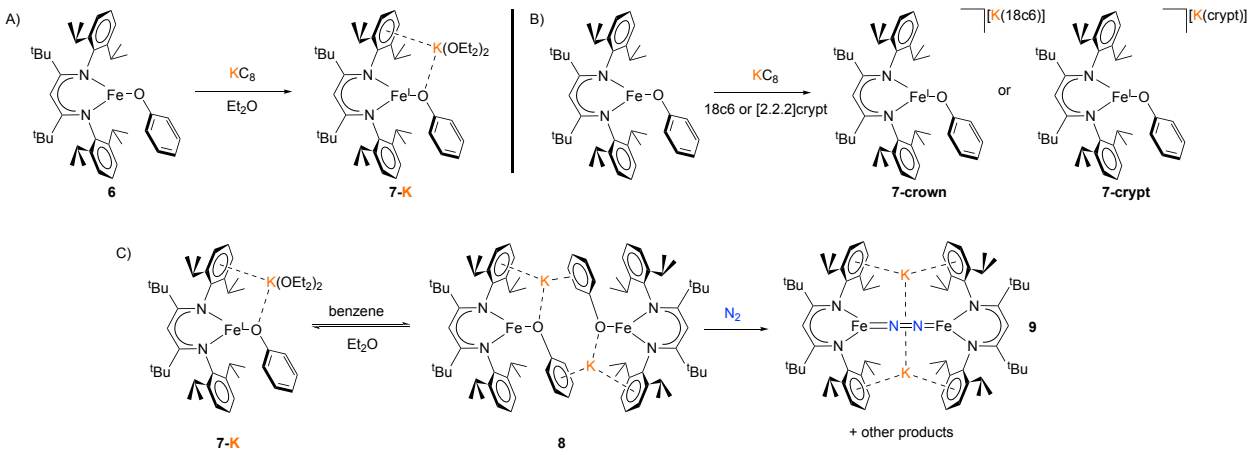

Scheme 4. Reactivity of iron–phenoxo complex **6** in the presence/absence of chelates and coordinating solvent.[27]

However, when **7-K** was dissolved in benzene (or if it was synthesized under conditions where there was no ether to complete the coordination sphere of K^+), the iron(I) phenoxide existed as the dimeric complex **8**, in which the K^+ forms bridges by binding to the phenoxide oxygen and to arenes. This structure was more reactive: under an atmosphere of N_2, **8** reacted at room temperature to form a bridging N_2 species **9**. Thus, N_2 binding required the bimetallic unit in **8**, as the monomeric analogues **7** did not bind N_2. Computational studies supported this idea, showing that both **7** and **8** can weakly bind N_2 in a terminal fashion, but **8** has the flexibility to reach a geometry in which N_2 can bridge the metals and initiate KOPh loss. Mindiola and coworkers subsequently reported another iron system, with pyridinedipyrrolyl ligands, in which pre-organization not only enabled N_2 binding but also led to an unusual bent FeNNFe core.[28] Thus, AM cations can be used to pre-organize reactive metal centers and prime them for reactivity.

Alkali Metal Cation Effects on N–N Bond Cleavage

Not only can AM cations influence N_2 binding, they can play a crucial role in the cleavage of the N–N bond of N_2. This can be likened to the beneficial roles of AM promoters such as K^+ in the HB process.[13] Furthermore, kinetic studies have shown that adsorbed N_2 dissociates to two nitrides in the rate-limiting step in catalysis on single crystal Fe catalysts, and a similar mechanism is likely operative on the Mittasch catalyst (porous Fe with Al and K oxides) that is used in industry.[9] Aluminum is considered to be a structural promoter that increases the surface area of the catalyst and provides more stability while potassium is regarded as an electronic promoter on the catalyst's surface. This effect is most often understood through Coulombic attraction of electrons in the solid toward the K^+. The desire to test this idea motivated us to explore the roles of AM^+ during N_2 activation in well-characterized iron complexes.

The most relevant system utilized a β-diketiminate ligand with smaller xylyl groups, which enables the iron atoms to more closely approach one another. The reduction of an iron(II) chloride dimer (**10**) with 2 equiv of Na^0, K^0, or Rb^0 led to a spectacular reaction in which one molecule of N_2 was reduced completely to nitrides by four Fe atoms.[10] The tetrairon bis(nitride) complex **12** was isolated, and Mössbauer studies showed that the oxidation states of the Fe sites were as shown in **Scheme 5**. The N–N bond was completely cleaved, and addition of acid gave high yields of ammonia (>80%). The N–N cleavage required the AM, and when 18-crown-6 was included, cleavage did not occur.

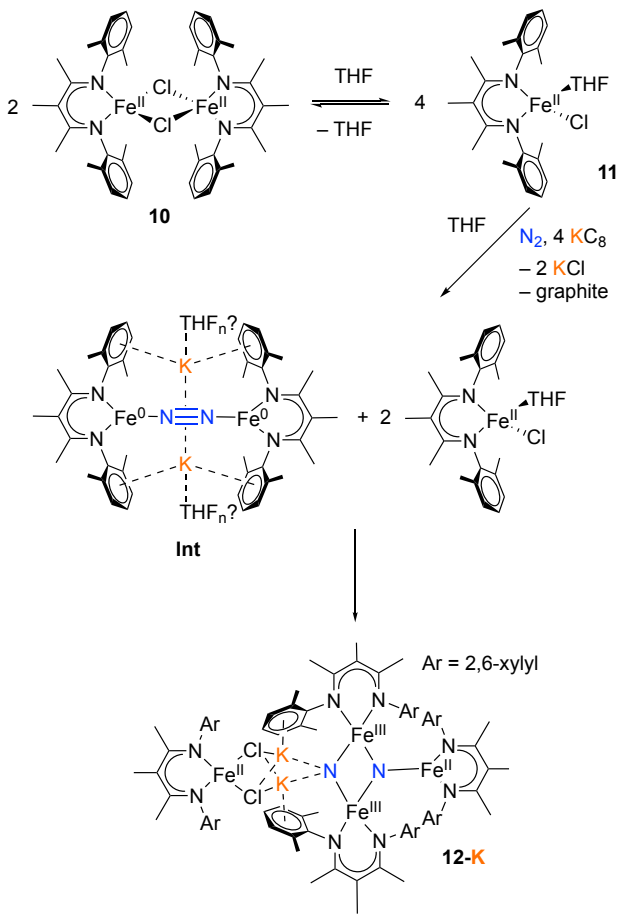

Scheme 5. Formation of bis-nitride product **12** from cleavage of N_2. Though analogues of **12** with Na^+ and Rb^+ were synthesized (see Scheme 6), the intermediates were explored spectroscopically only for K^+.[2,29]

To further understand the interplay between β-diketiminate–iron complexes and AM cations in N_2 reduction, we systematically studied the behavior of complex **10** with AM reductants (Na^0, KC_8, RbC_8, CsC_8).[2] Specifically, we treated **10** with 2 equivalents of RbC_8. Indeed, we obtained a bis-nitride product (**12-Rb**) with two Rb cations incorporated into the complex (**Scheme 6**). In the Rb analogue, the metrical parameters for the Fe_3N_2 core are indistinguishable from those of the K compound; however, the Rb–N distances are shorter. The observed shorter Rb–N distances may be due to rubidium's larger ionic radius, which causes longer bonds between the Rb and the π-

system, forcing the cation closer to the nitride. Changing the reductant to Na^0 (2 equivalents) yielded the tri-iron species (**12-Na**), which lacks the fourth, tetrahedral Fe site present in both the K and Rb species and contains only one cation.

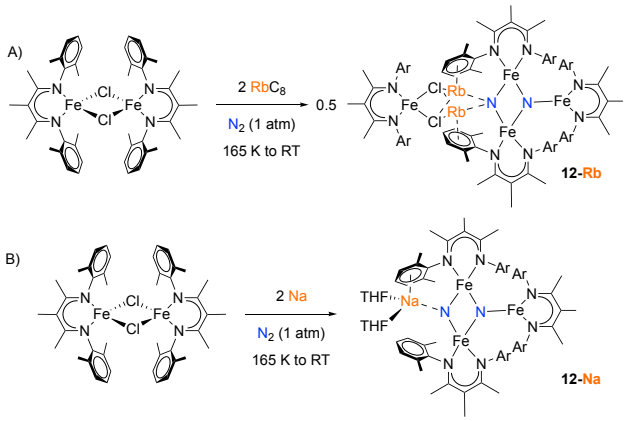

Scheme 6. Reduction of **10** to cleave N_2 and form **12-Rb** and **12-Na**.[2]

Using two equivalents of CsC_8 per iron did not give the analogous Cs bis-nitride species but instead furnished a trinuclear complex containing two bridging N_2 and a bridging chloride (**13**). This led us to treat **10** with 4 equiv of various AMC_8 (AM = K, Rb, or Cs), which in each case provided isolable triiron complexes **14-AM**, where the three iron sites are bridged by three N_2 bridges (**Scheme 7**). Crucial to their cores are two AM^+, above and below the $Fe_3(\mu\text{-}N_2)_3$ plane, which interact with the N_2 bridges and also have cation-π interactions with the β-diketiminate aryl groups. It is interesting that the use of *more* reductant led to *less* tendency to cleave N_2. This was another clear sign that the role of the AM was not just reduction: the number of AM cations in the products steers the reaction pathway to produce differently-shaped molecules.

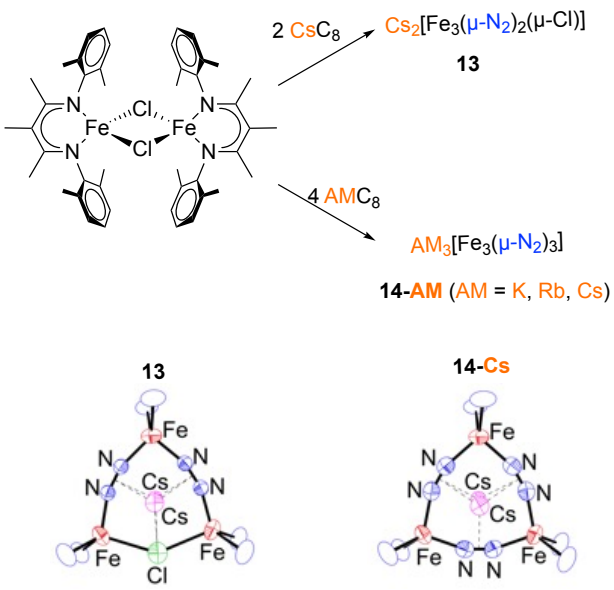

Scheme 7. Formation of trinuclear dinitrogen bridged complexes. Top view of complexes **13** and **14-Cs** with two cations occupying positions above and below the Fe-N_2 belt. **14-K** and **14-Rb** are isostructural to **14-Cs.** β-diketiminate ligands are omitted for clarity. Thermal ellipsoids are drawn at 50% probability.[2]

Aspects of the mechanism through which the N–N cleavage occurs were elucidated using DFT computations and high-level spectroscopy.[29,30] Initial DFT investigations focused on understanding how cooperative binding and K^+ affected the thermodynamics of N_2 cleavage. The calculations implicated a trimetallic iron intermediate wherein three reduced iron centers are necessary for cooperative binding of N_2, generating an Fe_3N_2 core (**Figure 4**). The N_2 binding mode with the iron centers is best described as end-on/end-on/side-on. When an electron was added to the Fe_3N_2 model, it resulted in a minimal geometric distortion. However, when an electron *and* K^+ are included, the rearrangement to the N–N bond cleaved bis-nitride structure on the right is favored. Importantly, the K^+ stabilized the bis-nitride, likely due to strong interactions with the anionic core. In further studies, Mössbauer, X-ray emission, X-ray absorption, and nuclear

resonance vibrational spectroscopies were used to gain experimental evidence for intermediates, accompanied by DFT computations on full models. While the complexity of the system hindered analysis (the precursor undergoes structural changes immediately upon dissolution), the evidence strongly suggested that a diiron(0) core is present in a transient intermediate **Int** (**Scheme 5**).

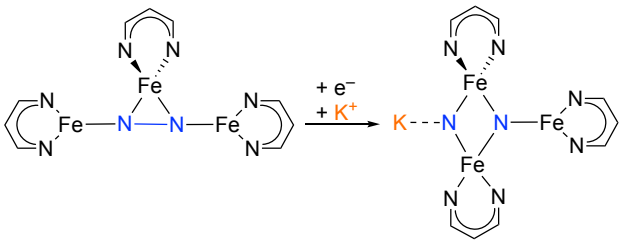

Figure 4. Depiction of multimetallic cooperativity involved in N_2 reduction in the presence of K^+. β-diketiminate ligands were modeled as $C_3N_2H_5^-$.[30]

Cooperative N–N bond cleavage is not limited to transition metal–dinitrogen complexes. For example, Mazzanti and co-workers have reported the reduction of a uranium(IV)–oxo complex with AMC_8 (AM = K, Rb, Cs) to furnish a series of uranium(III)–N_2 complexes.[31] The cation size affected the N_2 binding strength at room temperature and 1 atm: the K^+ analog bound N_2 strongly, binding was reversible with Rb^+, and no measurable binding was observed for Cs^+. Upon further reduction, all three complexes cleaved N_2 into two nitrides; however, only the Cs^+ analogue was isolable.

We note that AM cations can also affect the reactivity of β-diketiminate complexes with other small molecules as well. Driess and co-workers published a β-diketiminate–Ni superoxo complex that can be reduced to a peroxo species with K^0.[32] The resulting peroxo moiety exhibits an η^2 interaction with the K^+. When the K^+ is exchanged for Zn^{2+}, the O–O bond is cleaved. DFT calculations revealed the reactivity difference arises from different spin states as K^+ stabilizes a

singlet ground-state, while Zn^{2+} favors the triplet. Overall, a theme emerges: both the identity of the AM cation and the amount of reductant used impact the splitting of N–N and O–O bonds, typically involving interactions with ligand backbones.

Alkali Metal Cation Effects on C–H and C–S Bond Cleavage

Beyond the effects on N_2 complexes, AM cations can be used for breaking other bonds as well. For example, we found that treatment of a (β-diketiminate)iron hydride dimer (**15**) with sodium *tert*-butylthiolate or sodium dodecanethiolate yielded an iron sulfide complex (**16-Na**) from C–S cleavage (**Scheme 8**).[33] Using lithium dodecanethiolate provides the analogous complex with lithium (**16-Li**); however, exposing the starting dimer to potassium dodecanethiolate does not furnish the potassium analogue. Additionally, premixing **15** with [2.2.2]-cryptand before any AM dodecanethiolate addition does not form any detectable amount of **16-AM**.

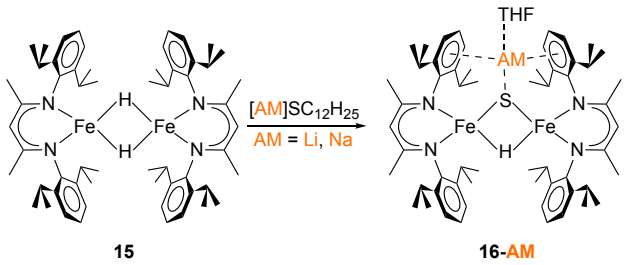

Scheme 8. Reaction of iron-hydride dimer **15** to form μ-sulfide **16** via C–S bond cleavage.[33,34]

Mechanistic investigations implicated a radical pathway involving C–S homolysis. These results suggest AM^+ interactions as an enabling factor in the reaction, but do not specify the precise way in which this occurs. We suggest two ways that the AM^+ could be affecting the reaction: pre-organization through cation–π interactions with the ligand or a thermodynamic effect due to stabilization of the incipient sulfide in the transition state.[34] In either case, the cation's ionic radius

impacts the AM cation's ability to fit between arenes of the β-diketiminate and interact with the complex's core. Perhaps Li^+ and Na^+ are small enough to form close contacts with the arenes and the bridging ligands in the diiron core, while K^+ may not be able to fit between the arenes to stabilize intermediates; alternatively, the necessary stabilization might require the greater Lewis acidity of the smaller AM cations.

Another influence on reactivity became apparent when the bis(nitride)tetrairon (**12-K**, discussed above) was treated with 18-crown-6. Removal of K^+ results in the formation of a triiron species (**17**) in which a benzylic proton has been transferred to give a μ-imido and form a new Fe–C bond (**Scheme 9**).[3]

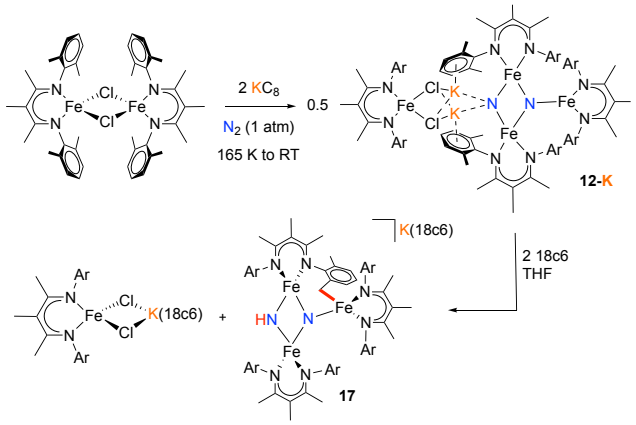

Scheme 9. Reactivity of **12-K** with 18-crown-6 to form **17**.[3]

This represented a surprising case of C–H activation induced by addition of a crown ether. To understand whether this effect was more general, a set of closely related (μ-imido)(μ-nitrido)triiron (**18**) and (μ-amido)(μ-nitrido)triiron (**20**) complexes was also reduced with KC_8 and subsequently treated with crown ether (**Scheme 10**). This treatment again resulted in deprotonation of a benzylic C–H and subsequent Fe–C bond formation to provide (μ-amido)(μ-nitrido)triiron and (μ-amido)(μ-imido)triiron complexes respectively. A possible mechanism is that removal of K^+ in

such reduced compounds uncovers a very basic bridging nitride or imide that can deprotonate the benzylic C–H bond of the supporting ligand. Overall, in the series of reactions, the K^+ is added to facilitate N–N cleavage and then removed to facilitate C–H cleavage, an intriguing example of AM control over difficult reactions.

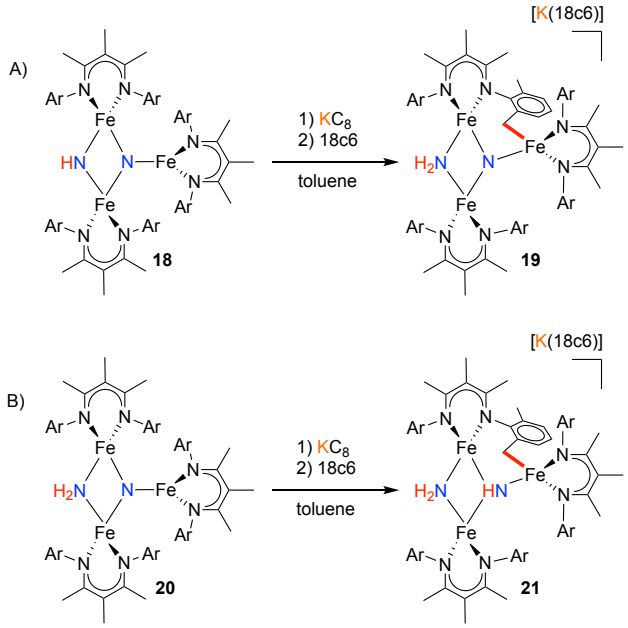

Scheme 10. Reactions testing the generality of benzylic deprotonation and Fe–C bond formation.[3]

A second example of AM influenced C–H activation was uncovered in more recent work from our group (**Scheme 11**). This was in the context of C–N bond formation from benzene and N_2 with an iron complex.[4] Reduction of **22** in the presence of benzene affords an iron(I) η^6-benzene complex (**23**). Upon further reduction, the iron activates the C–H bond of benzene (**25**). Interestingly, the C–H activation step has a marked dependence on the use of Na^+ vs. K^+. When the iron(I) η^6-benzene complex is treated with Na^0, a C–H bond of benzene undergoes oxidative addition to yield the iron(II) compound **25**. In contrast, treating the same iron(I) compound with KC_8 or RbC_8 gave an iron(0) benzene complex (**24**) without oxidative addition.[35] Importantly, addition of THF to either **24** or **25** gave a mixture of both iron(II) phenyl hydride and iron(0) benzene complexes,

suggesting that the C–H activation reaction is reversible. However, since **24** and **25** are isomers, the observation of interconversion implies that there is a thermodynamic bias induced by the specific choice of AM.

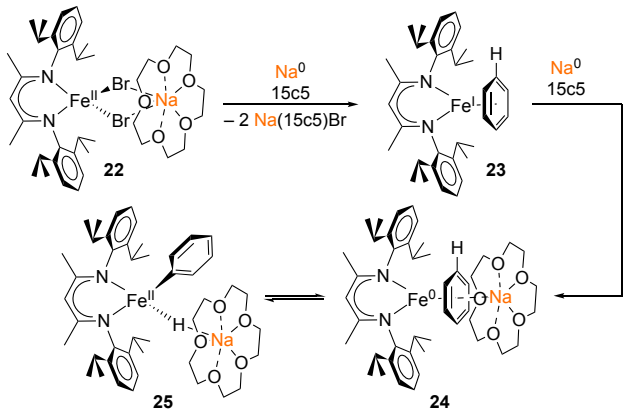

Scheme 11. Conversion of **22** to **25** through successive reductions and C–H activation.[4]

The sensitivity of these three compounds hindered attempts to experimentally determine equilibrium constants or to further test the AM^+ dependence of the equilibrium (**Scheme 12**). Thus, computational studies were used to interrogate the reasons for the AM^+ effect.[35] The analysis showed that electrostatic effects dominate in the case of Na^+, while steric effects dominate with the larger K^+ and Rb^+. Since the product has a shorter distance from AM^+ to the core of the iron complex, it is favored more by the use of Na^+. Likewise, since the transition state has a close approach of AM^+ to the core, the equilibrium is predicted to be more rapid for Na^+ than K^+ or Rb^+. Overall, this is an interesting example of AM influence on C–H activation, and it has promise for enabling selectivity when using anionic catalysts that attract AM^+ to the relevant species.

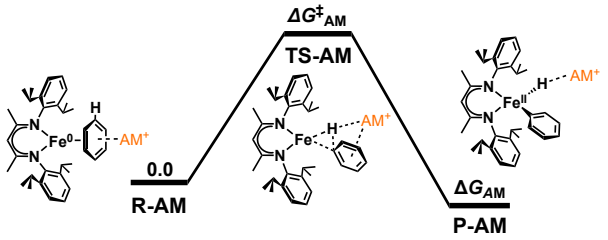

Alklai Cations (AM^+)	$\Delta G^{\ddagger}_{AM}$	ΔG_{AM}	Experimental equilibrium
no alkali cation	17.0	-2.2	equilibrium
$Na(15c5)^+$	15.1	-7.5	**P-Na** is dominant
$K(18c6)^+$	20.7	5.1	**R-K** is dominant
$Rb(18c6)^+$	20.9	4.8	**R-Rb** is dominant

Scheme 12. DFT-calculated free energy profile (in kcal/mol) of AM-tuned iron-mediated C–H activation in comparison with the experimental equilibrium. Reproduced from ref 35. Copyright 2025 American Chemical Society.

The Effect of Non-Covalent Interactions on Structure

Bridging carbonyls are well-known among low-spin, strong-field complexes, and AM^+ coordination to the bridging CO ligands is precedented.[36–42] However, the effect of AM cations on bridging CO in high-spin, weak-field complexes remains underexplored. Our group recently reported a high-spin β-diketiminate diiron system wherein bridging carbonyls were reduced in several steps.[43] This showed an important effect of AM^+ coordination on the π-accepting abilities of bridging carbonyls. Upon one-electron reduction of dicarbonyl complex **26** with KC_8 and [2.2.2]cryptand, a discrete cation-anion pair formed (**27-K**) (**Scheme 13**). The cation had no interaction with either carbonyl, and the ν_{CO} bands were observed at 1709 and 1619 cm^{-1}. However, when sodium naphthalenide ($NaC_{10}H_8$) in THF was used, **27-Na** was the product. This complex has one IR-active C–O stretching band at 1564 cm^{-1}, indicating higher symmetry in solution, likely due to Na^+ bridging CO units of adjacent complexes. Crystallization of **27-Na** from 2-

methyltetrahydrofuran (^{Me}THF) produced **27-^{Me}THF**, in which one CO coordinates to a Na(^{Me}THF)$_3^+$ cation while the other CO is "bare." The IR spectrum has bands at 1662 and 1588 cm^{-1}, and the lowering of one frequency is attributed to the interaction with Na$^+$.

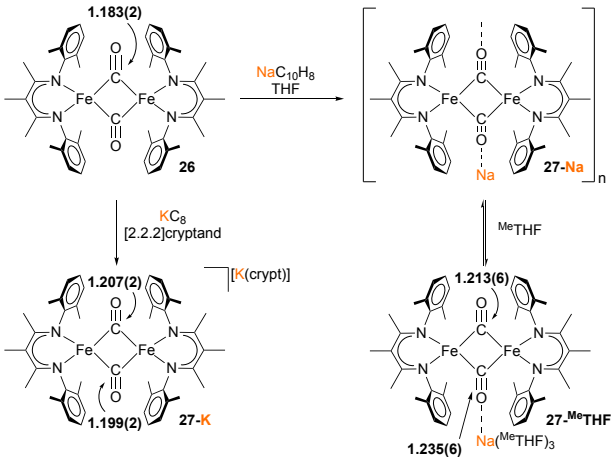

Scheme 13. Reduction of dicarbonyl compound **26** in the presence/absence of cryptand and coordinating solvent.[43]

Thus, Na$^+$ without coordinated solvent is able to withdraw more electron density into the bridging CO. The ν_{CO} dependence on solvent coordination to AM$^+$ is similar to $Fe_2(\mu\text{-}CO\text{–}Li(THF)_3)_2(CO)_6$, where THF-coordinated samples gave ν_{CO} of 1650 cm^{-1}, while removing THF shifted ν_{CO} to 1557 cm^{-1}.[39] Overall, the longer C–O bonds and lower energy IR bands that result when the carbonyls can interact with Na$^+$ demonstrate that AM cation coordination enhances the ability of CO to absorb electron density, though this effect is muffled somewhat when AM$^+$ has O-donors.

AM cation interactions with ligand backbones are not limited to the β-diketiminate systems described thus far. Indeed, any ligand containing a π-system has the possibility to form cation–π interactions. One such ligand is a formazanate, which is shaped similarly to a β-diketiminate ligand but has a more accessible LUMO making it easier to reduce to have radical character.[44,45] When AM metal reductants are used, the byproduct again contains an AM$^+$, which may or may not

interact with the transition-metal-containing product. Thus, the choice of AM offers an opportunity for modulating the properties. We began our investigations with the reduction of iron(II)–formazanate compound (**28**) with Na^0 with 12-crown-4, which resulted in **29** (**Scheme 14**).[46]

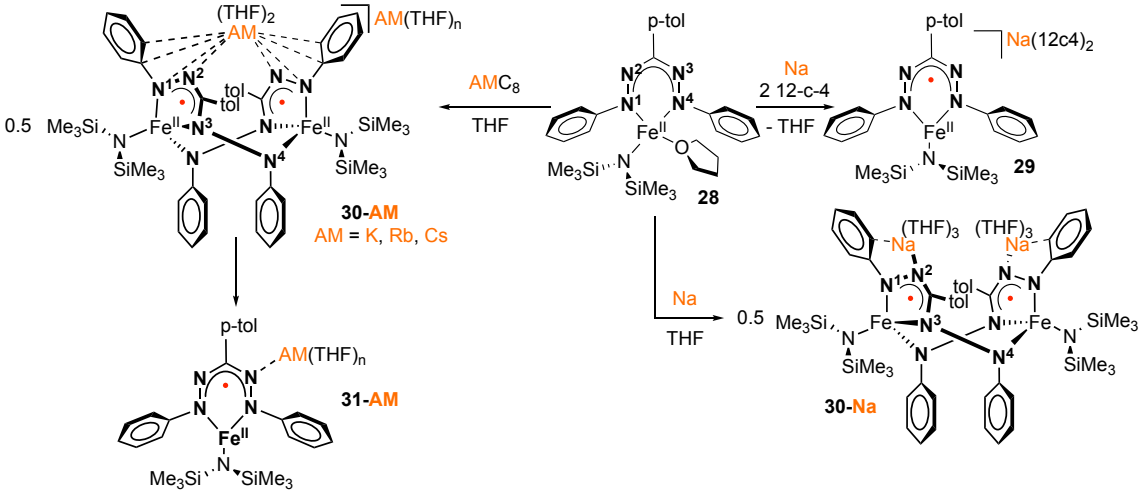

Scheme 14. Divergent reactivity of **28** upon reduction and exposure to crown ethers or coordinating solvent.[46,47]

In contrast to the β-diketiminate complexes described above, this product features a formazanate radical dianion and the iron remains iron(II) after reduction. In an interesting twist, reduction of the starting iron(II) complex without crown ether afforded dimeric **30-Na**, wherein the formazanate radical dianion rearranged to coordinate through N1 and N3 to form a five-membered chelate. The exocyclic nitrogen (N4) coordinates to the other Fe center in the dimer. As this rearrangement only occurs in the presence of unchelated AM cations, it is a clear example of an AM structural effect.

To further probe the change in binding mode, different AM sources (AMC_8, where AM = K, Rb, or Cs) were used.[47] Reduction of the starting iron(II)–formazanate with AMC_8 yielded similar dimeric compounds; however, the manner in which the AM cations are bound varied greatly

(**Figure 5**). Whereas each formazanate in the Na complex is bound to a single Na^+, in the K, Rb, and Cs analogues one AM cation bridges two formazanates.

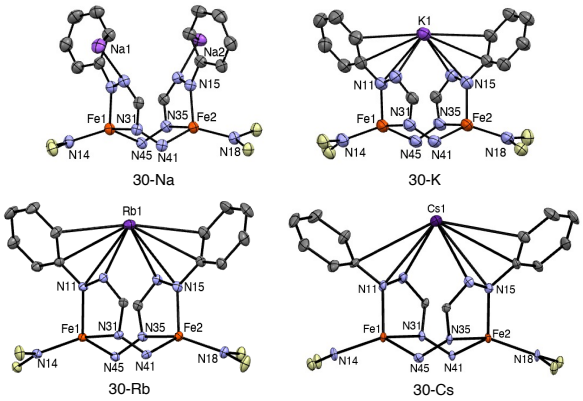

Figure 5. Displacement ellipsoid plots (drawn at 50%) of **30-Na, 30-K, 30-Rb,** and **30-Cs**, showing that the core structures change with different AM cations. Hydrogen atoms, selected organic fragments, and solvent molecules omitted for clarity. Reproduced from ref 47. Copyright 2018 American Chemical Society.

The formazanate binding mode in the dimeric complexes is stabilized by cation–π interactions with AM cations. As the ionic radius of the cation increases, the interplanar angle and distance between the five-membered metallacycles significantly increases. Additionally, the dimers convert to their corresponding monomers in THF solutions. Monitoring monomer formation by ^{1}H NMR shows the Cs analogue to be the fastest, followed by Rb and K. The periodic trend observed with K < Rb < Cs correlates with the cation *z/r* ratio (**Table 1** above), suggesting that smaller cations form stronger cation–π interactions in the starting material, which increases the activation barrier for isomerization and dimer splitting. However, the Na species was found to be faster than the K species, so this is not the only factor at play. It is possible that the different binding mode of the AM cations could play a role since each formazanate has an interaction with a separate cation in

the Na complex. Overall, these studies show how a ligand-centered reduction can act cooperatively with AM^+ coordination to result in transformations that may not have been possible had the metal center been reduced. The differences in ionic radii of AM cations lead to different stabilities of the dimers in solution corresponding to stronger interactions with smaller ions.

Alkali Metal Cation Effects on Relative d Orbital Energies

Most of the above effects involve AM^+ influencing the energies of compounds and transition states or of the positive charge on metal-ligand redox activity (such as backbonding into CO). In addition, newer efforts have started to elucidate AM^+ effects on the relative energies of d-orbitals at transition metal centers.[48] In our work, we have documented an SCS pincer-ligated iron complex where the specific location of a K^+ had a massive effect on the Mössbauer spectrum without changing the primary coordination geometry or the metal spin state. **Figure 6A-C** shows DFT-optimized structures of (SCS)Fe($N(SiMe_3)_2$ with inner-sphere K^+, with no cation, and with K(18-crown-6)$^+$. The distance of the cation to the core is most important because the electrostatic influence rearranges the d-orbital energies, causing the d_z^2 orbital and the d_{yz} orbital to change their occupations (**Figure 6D**). This in turn changes the electronic structure, causing the spectral shift.

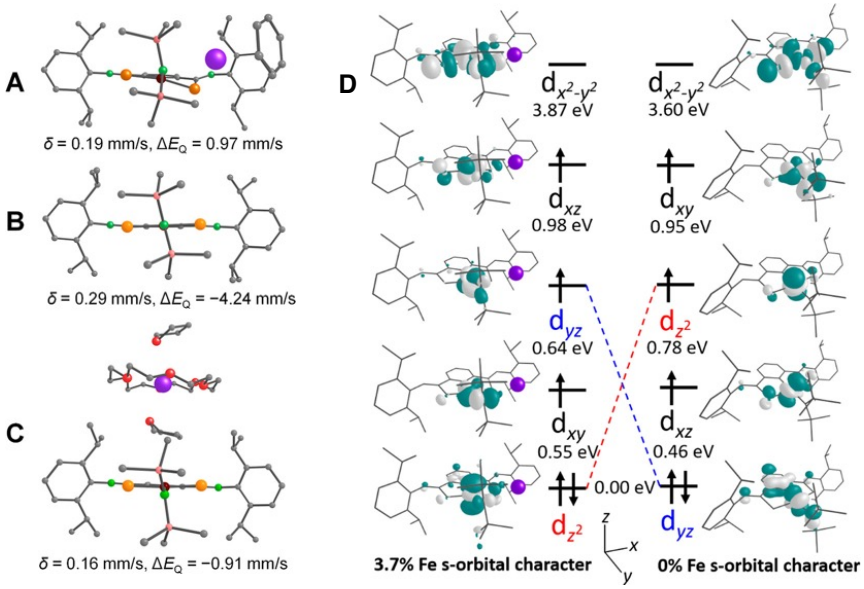

Figure 6. A-C Left: Optimized structures viewed along pincer plane with predicted Mössbauer parameters given below. (A) Optimized structure with K^+. (B) Optimized structure of anion without K^+. (C) Optimized structure with [K^+(18-crown-6)(THF)$_2$]. D Right: Relative energies of d-based orbitals along with plots of the quasi-restricted orbital plots at an isovalue of 0.03 au for the species in A (left) and B (right). Reproduced from ref 48. Copyright 2022 American Chemical Society.

This is not the only example of such an effect: Tomson and co-workers noted that phosphonium residues placed in the secondary coordination sphere of copper provided electrostatic stabilization of the d_z^2 orbital.[49] Additionally, the Yang group has reported the effect of alkali and alkaline earth metal cations on the orbital energies of iron and nickel salen complexes.[50] Overall, the presence of a cation can stabilize a nearby metal d-orbital, and the effect increases with greater positive charge. The impact of a positive charge near a transition metal center can be viewed as the reverse of a crystal-field model of negative charges around a metal, and it is natural that a nearby cation could bring about such an effect. These results suggest that there may be further opportunities for AM

effects in modulating orbital energies and controlling spins and magnetism, a future area about which chemists have only scratched the surface.

Summary

The use of AM cations to modulate reactivity represents a useful tool in a synthetic chemist's toolbox. The studies described above demonstrate how AM cations can interact with ancillary ligands, how they can affect the reactivity of TM complexes, and how they can impact electronic structures. One key parameter is the size of the AM cation. In several cases above (for example, the torsion angles of **2** and the bridging modes of **30**), varying the size of AM^+ caused significant structural changes. However, more often the primary impact of the size of AM^+ relates to the charge density, as the larger charge/size ratio of smaller AM^+ leads to stronger interactions. For example, formazanate dimers that were held together by alkali metals (**30–AM**) cleaved more slowly with smaller, charge-dense AM^+. In Schemes 5-7 it was shown that Na^+, K^+, and Rb^+ could cleave N_2, whereas the larger Cs^+ could not. In Scheme 8 it was shown that Li^+ and Na^+ could cleave C–S bonds, but the larger K^+ could not. In Scheme 12, Na^+ enhanced the rate and favorability of C–H activation, while K^+ and Rb^+ could not. All of these effects are attributable to the greater Lewis acidity of smaller AM cations. The charge effect can alter electronic structures, for example promoting backbonding with π-accepting ligands (Scheme 13) and differentially stabilizing iron *d* orbitals (Figure 6).

The Lewis acidity of a given AM^+ can be modulated through the use of Lewis basic donors, such as crown ethers or cryptands. Chelates most often increase the steric hindrance around the AM^+ cation and disrupt the interactions with π-systems of supporting ligands. For example, the FeNNFe

core in **2–K** is stable, but addition of 18-crown-6 disrupts the dimer, affording a more reactive terminal–N_2 complex.

An additional emergent theme is that AM^+ can play a structural role, holding supporting ligands in a geometry that encourages specific reactions. An example is the studies on iron-phenolate complexes (Scheme 4), in which N_2 reactivity became feasible only when the K^+ ions held the two metals in a specific orientation. Another example is the formation of unprecedented planar Fe_4S_3 clusters, which have cation-π interactions to K^+, Rb^+, or Cs^+ that hold the cluster in its triangular shape.[51] It is likely that the ability of the AM cations to hold the β-diketiminate ligands in the correct relative orientation is important for formation and stabilization of the unusual cluster shape.

In the future, we envision further use of AM cations to accelerate reactions in which electron density moves toward the ligand that interacts with AM^+. Examples above show the feasibility of this strategy for small-molecule activation reactions such as oxidative addition of C–H bonds, reduction of N_2, and reduction of CO. Other creative uses of this power will certainly emerge in the future. Additionally, AM^+ could be introduced externally rather than by use of a AM^0 reducing agent; this may require that the complex is anionic to give sufficient interaction with the weakly Lewis-acidic AM^+. However, Szymczak has shown that AM^+ can interact with a neutral Re–N_2 complex strongly enough to effect the N–N stretching frequency.[52]

We hope that the summary in this Account will inspire future chemistry, and we close by pointing out some inspirational work on AM^+-assisted small-molecule activation by other research groups. Smith has shown AM effects on the reactivity of an iron(II)-imido complexes.[53] Young has shown AM effects on C–halide activation in iron(0) complexes.[54] Limberg has systematically studied the effects of AM^+ on CO_2 activation by nickel complexes.[55] Hevia has shown AM effects on C–H

activation.[56] Overall, the study of AM effects is a vibrant area of current organometallic chemistry which has great promise for improving reactivity and selectivity.

Acknowledgments

This work was supported by the U.S. Department of Energy, Office of Science, Office of Basic Energy Sciences, Catalysis Science program, under Award DE-SC0020315.

References

(1) McWilliams, S. F.; Rodgers, K. R.; Lukat-Rodgers, G.; Mercado, B. Q.; Grubel, K.; Holland, P. L. Alkali Metal Variation and Twisting of the FeNNFe Core in Bridging Diiron Dinitrogen Complexes. *Inorg. Chem.* **2016**, *55* (6), 2960–2968. https://doi.org/10.1021/acs.inorgchem.5b02841.

(2) Grubel, K.; Brennessel, W. W.; Mercado, B. Q.; Holland, P. L. Alkali Metal Control over N–N Cleavage in Iron Complexes. *J. Am. Chem. Soc.* **2014**, *136* (48), 16807–16816. https://doi.org/10.1021/ja507442b.

(3) MacLeod, K. C.; Menges, F. S.; McWilliams, S. F.; Craig, S. M.; Mercado, B. Q.; Johnson, M. A.; Holland, P. L. Alkali-Controlled C–H Cleavage or N–C Bond Formation by N_2-Derived Iron Nitrides and Imides. *J. Am. Chem. Soc.* **2016**, *138* (35), 11185–11191. https://doi.org/10.1021/jacs.6b04984.

(4) McWilliams, S. F.; Broere, D. L. J.; Halliday, C. J. V.; Bhutto, S. M.; Mercado, B. Q.; Holland, P. L. Coupling Dinitrogen and Hydrocarbons through Aryl Migration. *Nature* **2020**, *584* (7820), 221–226. https://doi.org/10.1038/s41586-020-2565-5.

(5) Suelter, C. H. Enzymes Activated by Monovalent Cations. *Science* **1970**, *168* (3933), 789–795.

(6) Cera, E. D. A Structural Perspective on Enzymes Activated by Monovalent Cations. *Journal of Biological Chemistry* **2006**, *281* (3), 1305–1308. https://doi.org/10.1074/jbc.R500023200.

(7) Page, M. J.; Di Cera, E. Role of Na^+ and K^+ in Enzyme Function. *Physiological Reviews* **2006**, *86* (4), 1049–1092. https://doi.org/10.1152/physrev.00008.2006.

(8) Wang, J.; Boisvert, D. C. Structural Basis for GroEL-Assisted Protein Folding from the Crystal Structure of (GroEL-KMgATP)$_{14}$ at 2.0 Å Resolution. *Journal of Molecular Biology* **2003**, *327* (4), 843–855. https://doi.org/10.1016/S0022-2836(03)00184-0.

(9) Appl, M. Ammonia, 2. Production Processes. In *Ullmann's Encyclopedia of Industrial Chemistry*; John Wiley & Sons, Ltd, 2011. https://doi.org/10.1002/14356007.o02_o11.

(10) Rodriguez, M. M.; Bill, E.; Brennessel, W. W.; Holland, P. L. N_2 Reduction and Hydrogenation to Ammonia by a Molecular Iron-Potassium Complex. *Science* **2011**, *334* (6057), 780–783. https://doi.org/10.1126/science.1211906.

(11) Machado-Vieira, R.; Manji, H. K.; Zarate, C. A. The Role of Lithium in the Treatment of Bipolar Disorder: Convergent Evidence for Neurotrophic Effects as a Unifying Hypothesis. *Bipolar Disord* **2009**, *11* (Suppl 2), 92–109. https://doi.org/10.1111/j.1399-5618.2009.00714.x.

(12) Stambolic, V.; Ruel, L.; Woodgett, J. R. Lithium Inhibits Glycogen Synthase Kinase-3 Activity and Mimics Wingless Signalling in Intact Cells. *Current Biology* **1996**, *6* (12), 1664–1669. https://doi.org/10.1016/S0960-9822(02)70790-2.

(13) Connor, G. P.; Holland, P. L. Coordination Chemistry Insights into the Role of Alkali Metal Promoters in Dinitrogen Reduction. *Catalysis Today* **2017**, *286*, 21–40. https://doi.org/10.1016/j.cattod.2016.08.014.

(14) Xu, Y.; Xia, Z.; Gao, W.; Xiao, H.; Xu, B. Cation Effect on the Elementary Steps of the Electrochemical CO Reduction Reaction on Cu. *Nat. Catal.* **2024**, *7* (10), 1120–1129. https://doi.org/10.1038/s41929-024-01227-z.

(15) Zhang, Z.; Li, H.; Shao, Y.; Gan, L.; Kang, F.; Duan, W.; Hansen, H. A.; Li, J. Molecular Understanding of the Critical Role of Alkali Metal Cations in Initiating CO_2 Electroreduction on Cu(100) Surface. *Nat Commun* **2024**, *15* (1), 612. https://doi.org/10.1038/s41467-024-44896-x.

(16) González-Riopedre, G.; Bermejo, M. R.; Fernández-García, M. I.; González-Noya, A. M.; Pedrido, R.; Rodríguez-Doutón, M. J.; Maneiro, M. Alkali-Metal-Ion-Directed Self-Assembly of Redox-Active Manganese(III) Supramolecular Boxes. *Inorg. Chem.* **2015**, *54* (6), 2512–2521. https://doi.org/10.1021/ic501842x.

(17) Acosta-Calle, S.; Miller, A. J. M. Tunable and Switchable Catalysis Enabled by Cation-Controlled Gating with Crown Ether Ligands. *Acc. Chem. Res.* **2023**, *56* (8), 971–981. https://doi.org/10.1021/acs.accounts.3c00056.

(18) Reath, A. H.; Ziller, J. W.; Tsay, C.; Ryan, A. J.; Yang, J. Y. Redox Potential and Electronic Structure Effects of Proximal Nonredox Active Cations in Cobalt Schiff Base Complexes. *Inorg. Chem.* **2017**, *56* (6), 3713–3718. https://doi.org/10.1021/acs.inorgchem.6b03098.

(19) Holland, P. L. Electronic Structure and Reactivity of Three-Coordinate Iron Complexes. *Acc. Chem. Res.* **2008**, *41* (8), 905–914. https://doi.org/10.1021/ar700267b.

(20) Hasanayn, F.; Holland, P. L.; Goldman, A. S.; Miller, A. J. M. Lewis Structures and the Bonding Classification of End-on Bridging Dinitrogen Transition Metal Complexes. *J. Am. Chem. Soc.* **2023**, *145* (8), 4326–4342. https://doi.org/10.1021/jacs.2c12243.

(21) Shannon, R. D. Revised Effective Ionic Radii and Systematic Studies of Interatomic Distances in Halides and Chalcogenides. *Acta Crystallographica Section A* **1976**, *32* (5), 751–767. https://doi.org/10.1107/S0567739476001551.

(22) Horn, B.; Pfirrmann, S.; Limberg, C.; Herwig, C.; Braun, B.; Mebs, S.; Metzinger, R. N_2 Activation in Ni^{I}–NN–Ni^{I} Units: The Influence of Alkali Metal Cations and CO Reactivity. *Zeitschrift für anorganische und allgemeine Chemie* **2011**, *637* (9), 1169–1174. https://doi.org/10.1002/zaac.201100140.

(23) Ding, K.; Pierpont, A. W.; Brennessel, W. W.; Lukat-Rodgers, G.; Rodgers, K. R.; Cundari, T. R.; Bill, E.; Holland, P. L. Cobalt−Dinitrogen Complexes with Weakened N−N Bonds. *J. Am. Chem. Soc.* **2009**, *131* (27), 9471–9472. https://doi.org/10.1021/ja808783u.

(24) Pedersen, C. J. Cyclic Polyethers and Their Complexes with Metal Salts. *J. Am. Chem. Soc.* **1967**, *89* (26), 7017–7036. https://doi.org/10.1021/ja01002a035.

(25) Gokel, G. W.; Korzeniowski, S. H. Cryptands and Related Polycyclic Systems. In *Macrocyclic Polyether Syntheses*; Gokel, G. W., Korzeniowski, S. H., Eds.; Springer: Berlin, Heidelberg, 1982; pp 347–394. https://doi.org/10.1007/978-3-642-68451-7_8.

(26) McWilliams, S. F.; Bill, E.; Lukat-Rodgers, G.; Rodgers, K. R.; Mercado, B. Q.; Holland, P. L. Effects of N_2 Binding Mode on Iron-Based Functionalization of Dinitrogen to Form an Iron(III) Hydrazido Complex. *J. Am. Chem. Soc.* **2018**, *140* (27), 8586–8598. https://doi.org/10.1021/jacs.8b04828.

(27) Chiang, K. P.; Bellows, S. M.; Brennessel, W. W.; Holland, P. L. Multimetallic Cooperativity in Activation of Dinitrogen at Iron–Potassium Sites. *Chem. Sci.* **2014**, *5* (1), 267–274. https://doi.org/10.1039/C3SC52487F.

(28) Sorsche, D.; Miehlich, M. E.; Searles, K.; Gouget, G.; Zolnhofer, E. M.; Fortier, S.; Chen, C.-H.; Gau, M.; Carroll, P. J.; Murray, C. B.; Caulton, K. G.; Khusniyarov, M. M.; Meyer, K.; Mindiola, D. J. Unusual Dinitrogen Binding and Electron Storage in Dinuclear Iron Complexes. *J. Am. Chem. Soc.* **2020**, *142* (18), 8147–8159. https://doi.org/10.1021/jacs.0c01488.

(29) Wandzilak, A.; Grubel, K.; Skubi, K. L.; McWilliams, S. F.; Bessas, D.; Rana, A.; Hugenbruch, S.; Dey, A.; Holland, P. L.; DeBeer, S. Mössbauer and Nuclear Resonance Vibrational Spectroscopy Studies of Iron Species Involved in N–N Bond Cleavage. *Inorg. Chem.* **2023**, *62* (45), 18449–18464. https://doi.org/10.1021/acs.inorgchem.3c02594.

(30) Figg, T. M.; Holland, P. L.; Cundari, T. R. Cooperativity Between Low-Valent Iron and Potassium Promoters in Dinitrogen Fixation. *Inorg. Chem.* **2012**, *51* (14), 7546–7550. https://doi.org/10.1021/ic300150u.

(31) Jori, N.; Rajeshkumar, T.; Scopelliti, R.; Ivković, I.; Sienkiewicz, A.; Maron, L.; Mazzanti, M. Cation Assisted Binding and Cleavage of Dinitrogen by Uranium Complexes. *Chem. Sci.* **2022**, *13* (32), 9232–9242. https://doi.org/10.1039/D2SC02530B.

(32) Yao, S.; Xiong, Y.; Vogt, M.; Grützmacher, H.; Herwig, C.; Limberg, C.; Driess, M. O–O Bond Activation in Heterobimetallic Peroxides: Synthesis of the Peroxide [LNi(μ-η^2:η^2-O_2)K] and Its Conversion into a Bis(μ-Hydroxo) Nickel Zinc Complex. *Angewandte Chemie International Edition* **2009**, *48* (43), 8107–8110. https://doi.org/10.1002/anie.200903772.

(33) Arnet, N. A.; Dugan, T. R.; Menges, F. S.; Mercado, B. Q.; Brennessel, W. W.; Bill, E.; Johnson, M. A.; Holland, P. L. Synthesis, Characterization, and Nitrogenase-Relevant Reactions of an Iron Sulfide Complex with a Bridging Hydride. *J. Am. Chem. Soc.* **2015**, *137* (41), 13220–13223. https://doi.org/10.1021/jacs.5b06841.

(34) Arnet, N. A.; McWilliams, S. F.; DeRosha, D. E.; Mercado, B. Q.; Holland, P. L. Synthesis and Mechanism of Formation of Hydride–Sulfide Complexes of Iron. *Inorg. Chem.* **2017**, *56* (15), 9185–9193. https://doi.org/10.1021/acs.inorgchem.7b01230.

(35) Li, Y.; Hidalgo, N.; Bhutto, S. M.; Chew, N. B.; Mercado, B. Q.; Holland, P. L.; Chen, H. Alkali Metal Control of Triplet-Mediated C–H Activation in Iron-Mediated Coupling of Dinitrogen and Benzene. *Inorg. Chem.* **2025**, *64* (34), 17387–17398. https://doi.org/10.1021/acs.inorgchem.5c02695.

(36) Braterman, P. S. Spectra and Bonding in Metal Carbonyls, Part A: Bonding. In *Structure and Bonding*; Springer Berlin Heidelberg: Berlin, Heidelberg, 1972; pp 57–86.

(37) Braterman, P. S. Spectra and Bonding in Metal Carbonyls Part B: Spectra and Their Interpretation. In *Spectra and Chemical Interactions*; Braterman, P. S., Blasse, G., Müller, A., Baran, E. J., Carter, R. O., Eds.; Springer Berlin Heidelberg: Berlin, Heidelberg, 1976; pp 1–42.

(38) Heijser, W.; Baerends, E. J.; Ros, P. Electronic Structure of Binuclear Metal Carbonyl Complexes. *Faraday Symp. Chem. Soc.* **1980**, *14* (0), 211–234. https://doi.org/10.1039/FS9801400211.

(39) Neumüller, B.; Petz, W. Reaction of $Fe_2(CO)_9$ with Lithium: Preparation and Structures of Compounds with Strong Ion Pairing. *Organometallics* **2001**, *20* (1), 163–170. https://doi.org/10.1021/om000597r.

(40) Hu, N.; Nie, G.; Jin, Z.; Chen, W. Crystal Structures of Bis(Cyclopentadienyldicarbonyliron)Sodium Tetrahydrofuran and (Cyclopentadienyldicarbonyliron)Sodium Tetramethylethylenediamine Complexes. *Journal of*

Organometallic Chemistry **1989**, *377* (1), 137–143. https://doi.org/10.1016/0022-328X(89)80059-2.

(41) Blake, M. P.; Kaltsoyannis, N.; Mountford, P. Probing the Limits of Alkaline Earth–Transition Metal Bonding: An Experimental and Computational Study. *J. Am. Chem. Soc.* **2015**, *137* (38), 12352–12368. https://doi.org/10.1021/jacs.5b07866.

(42) Kückmann, T. I.; Bolte, M.; Wagner, M.; Lerner, H.-W. Adducts of $NaOSiMePh_2$ Oligomers with THF and Cyclopentadienyl Iron Dicarbonyl Dimer. *Zeitschrift für anorganische und allgemeine Chemie* **2007**, *633* (2), 290–297. https://doi.org/10.1002/zaac.200600281.

(43) Nagelski, A. L.; Fataftah, M. S.; MacMillan, S. N.; MacLeod, K. C.; McWilliams, S. F.; Mercado, B. Q.; Lancaster, K. M.; Holland, P. L. Bridging Carbonyl and Carbyne Complexes of Weak-Field Iron: Electronic Structure and Iron–Carbon Bonding. *J. Am. Chem. Soc.* **2024**, *146* (47), 32415–32430. https://doi.org/10.1021/jacs.4c08358.

(44) Chang, M.-C.; Dann, T.; Day, D. P.; Lutz, M.; Wildgoose, G. G.; Otten, E. The Formazanate Ligand as an Electron Reservoir: Bis(Formazanate) Zinc Complexes Isolated in Three Redox States. *Angewandte Chemie International Edition* **2014**, *53* (16), 4118–4122. https://doi.org/10.1002/anie.201309948.

(45) Milocco, F.; Demeshko, S.; Meyer, F.; Otten, E. Ferrate(II) Complexes with Redox-Active Formazanate Ligands. *Dalton Trans.* **2018**, *47* (26), 8817–8823. https://doi.org/10.1039/C8DT01597J.

(46) Broere, D. L. J.; Mercado, B. Q.; Lukens, J. T.; Vilbert, A. C.; Banerjee, G.; Lant, H. M. C.; Lee, S. H.; Bill, E.; Sproules, S.; Lancaster, K. M.; Holland, P. L. Reversible Ligand-Centered Reduction in Low-Coordinate Iron Formazanate Complexes. *Chemistry – A European Journal* **2018**, *24* (37), 9417–9425. https://doi.org/10.1002/chem.201801298.

(47) Broere, D. L. J.; Mercado, B. Q.; Bill, E.; Lancaster, K. M.; Sproules, S.; Holland, P. L. Alkali Cation Effects on Redox-Active Formazanate Ligands in Iron Chemistry. *Inorg. Chem.* **2018**, *57* (16), 9580–9591. https://doi.org/10.1021/acs.inorgchem.8b00226.

(48) Skubi, K. L.; Hooper, R. X.; Mercado, B. Q.; Bollmeyer, M. M.; MacMillan, S. N.; Lancaster, K. M.; Holland, P. L. Iron Complexes of a Proton-Responsive SCS Pincer Ligand with a Sensitive Electronic Structure. *Inorg. Chem.* **2022**, *61* (3), 1644–1658. https://doi.org/10.1021/acs.inorgchem.1c03499.

(49) Weberg, A. B.; McCollom, S. P.; Thierer, L. M.; Gau, M. R.; Carroll, P. J.; Tomson, N. C. Using Internal Electrostatic Fields to Manipulate the Valence Manifolds of Copper Complexes. *Chem. Sci.* **2021**, *12* (12), 4395–4404. https://doi.org/10.1039/D0SC06364A.

(50) Kang, K.; Fuller, J.; Reath, A. H.; Ziller, J. W.; Alexandrova, A. N.; Yang, J. Y. Installation of Internal Electric Fields by Non-Redox Active Cations in Transition Metal Complexes. *Chem. Sci.* **2019**, *10* (43), 10135–10142. https://doi.org/10.1039/C9SC02870F.

(51) DeRosha, D. E.; Chilkuri, V. G.; Van Stappen, C.; Bill, E.; Mercado, B. Q.; DeBeer, S.; Neese, F.; Holland, P. L. Planar Three-Coordinate Iron Sulfide in a Synthetic [4Fe-3S] Cluster with Biomimetic Reactivity. *Nat. Chem.* **2019**, *11* (11), 1019–1025. https://doi.org/10.1038/s41557-019-0341-7.

(52) Shanahan, J. P.; Szymczak, N. K. Hydrogen Bonding to a Dinitrogen Complex at Room Temperature: Impacts on N_2 Activation. *J. Am. Chem. Soc.* **2019**, *141* (21), 8550–8556. https://doi.org/10.1021/jacs.9b02288.

(53) Gao, Y.; Pink, M.; Smith, J. M. Alkali Metal Ions Dictate the Structure and Reactivity of an Iron(II) Imido Complex. *J. Am. Chem. Soc.* **2022**, *144* (4), 1786–1794. https://doi.org/10.1021/jacs.1c11429.

(54) Ji, S. G.; Kim, M. M.; Han, M. H.; Cho, J.; Son, Y.; Kim, Y. Y.; Jeong, J.; Kim, Z. H.; Chae, K. H.; Oh, H.-S.; Kim, H.; Choi, C. H. Alkali Metal Cations Act as Homogeneous Cocatalysts for the Oxygen Reduction Reaction in Aqueous Electrolytes. *Nat Catal* **2024**, *7* (12), 1330–1338. https://doi.org/10.1038/s41929-024-01241-1.

(55) Wolff, S.; Pelmenschikov, V.; Müller, R.; Ertegi, M.; Cula, B.; Kaupp, M.; Limberg, C. Controlling the Activation at Ni^{II}–CO_2^{2-} Moieties through Lewis Acid Interactions in the Second Coordination Sphere. *Chemistry – A European Journal* **2024**, *30* (18), e202303112. https://doi.org/10.1002/chem.202303112.

(56) Maddock, L. C. H.; Mu, M.; Kennedy, A. R.; García-Melchor, M.; Hevia, E. Facilitating the Ferration of Aromatic Substrates through Intramolecular Sodium Mediation. *Angewandte Chemie International Edition* **2021**, *60* (28), 15296–15301. https://doi.org/10.1002/anie.202104275.